THZ IMAGING BY A WIDE-BAND COMPACT FEL

Young Uk Jeong, Hyuk Jin Cha, Seong Hee Park, Byung Cheol Lee, KAERI, Daejon, Korea
Grigori M. Kazakevitch, BINP, Novosibirsk, Russia

Abstract

We have developed a laboratory-scale users facility with a compact terahertz (THz) free electron laser (FEL). The FEL operates in the wavelength range of 100–1200 μm, which corresponds to 0.3–3 THz. THz radiation from the FEL shows well collimated Gaussian spatial distribution and narrow spectral width of $\Delta\lambda/\lambda \sim 0.003$, which is Fourier transform limited by the estimated pulse duration of 20 ps. The main application of the FEL is THz imaging for bio-medical researches. We are developing THz imaging techniques by 2-dimensional (2-D) scanning, single pulse capturing with the electro-optic method, and 3-D holography. High power, coherent, and short-pulsed feature of the FEL radiation is expected to show much better performance in advanced THz imaging of 3-D tomography. The coherent length of the FEL micropulse is measured to be 8-12 mm. In this paper we will show and discuss the main results of THz imaging with the different methods by using the KAERI compact FEL.

INTRODUCTION

T-ray which means THz radiation imaging technology was selected as one of '10 emerging technologies that will change your world' by a magazine named MIT's Technology Review of January 31, 2004. If we see the other selected technologies, e.g. universal translation, synthetic biology, and so on, the potentiality of the THz radiation technology might go beyond the usual understanding of us. THz radiation has several remarkable advantages for imaging compared with other conventional sources, such as safe energy range without ionization to the materials, foot-print spectral region of most chemicals and bio-materials, and relatively high spatial resolution for medical imaging.

There are several kinds of THz radiation sources [1–5]. Table-top THz sources generated by conventional lasers have been developed and used for various applications in the THz range [6–8]. However, advanced THz imaging such as tomography of living species requires much more power of the radiation to get information with better S/N ratio and higher speed of data acquisition. Inexpensive and compact THz FEL [5,9] can play the important role of encouraging the advanced THz applications due to its higher power and spectral brightness compared to the table-top sources.

We have developed a THz users facility based on a compact FEL [10]. The wavelength range of the FEL is 100-1000 μm and we could construct a users experimental stage for the wavelength of 100–300 μm. The THz FEL beam shows good performance in pulse-energy stability, polarization, spectrum and spatial distribution. We could get the 2-D imaging of various materials with the THz FEL beam. The measured coherence length of the THz FEL micropulses is 8-12 mm, which corresponds to 25-40 ps. The main idea for 3-D coherent THz tomography with the coherent pulse is proposed and discussed in this paper.

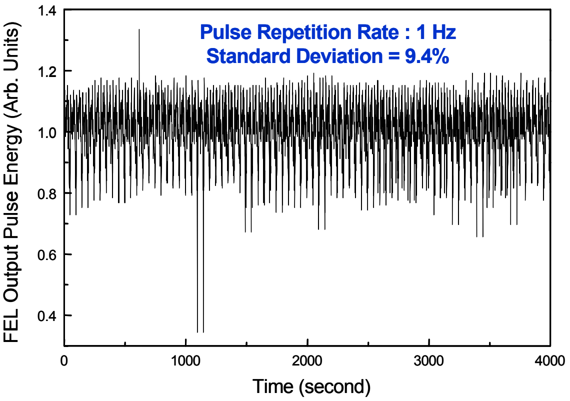

Figure 1: Measured fluctuation of the THz pulse energy depending on time.

THZ FEL BEAM CHARACTERISTICS FOR IMAGING

The stability of the radiation pulse energy was improved by keeping cooling water and air temperature of the system and laboratory within 0.1 and 1^{O}C, respectively. Figure 1 shows the measured fluctuation of the THz pulse energy depending on time. The repetition rate of the FEL macropulse was 1 Hz during the measurement. We could not observe any drift of average value of the FEL pulse energy and the fluctuation of the pulse energy is less than 10% in r.m.s value. If we monitor and normalize the pulse energy fluctuation of the FEL beam, the measuring error is decreased to be less than 1%. With the stable THz pulses, we could measure 2-D scanned imaging, interference patterns, or spectroscopic information of species with high resolution.

The polarization of the THz FEL beam has been measured by using a metal-wire polarizer having 20 μm spacing, which is shown in Fig. 2. The FEL beam is highly polarized with a linear component of more than 98% due to wiggling motion of the electron beam inside a planar undulator. We could understand that the polarization of the FEL beam is not disturbed by the long distance (~10 m) propagation with more than 10 pieces of mirrors, windows and lens.

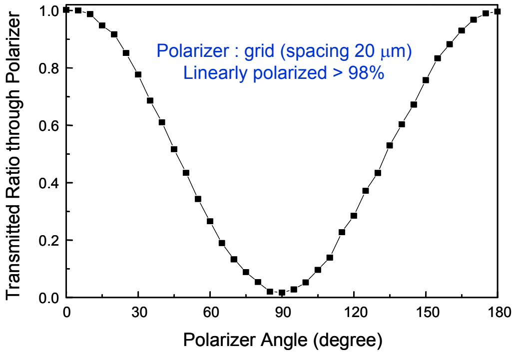

Figure 2: Measured polarization of the THz FEL beam by using a metal-wire polarizer having 20 μm spacing.

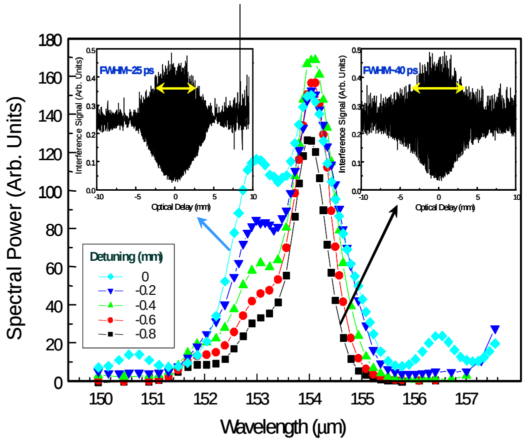

Figure 3: Measured FEL beam spectra depending on detuning lengths of the FEL cavity. Measured results of the coherence lengths of the FEL micro-bunches for the detuning lengths of 0 and -0.8 mm from the resonance position of the FEL optical cavity are shown in left and right insets of the figure, respectively.

Spectra of the FEL beam have been measured by a high resolution spectrometer having resolution of 10^{-4}. And the results were compared by the measured value of the coherence length of the FEL micropulses. Coherent length of the FEL micropulse could be measured by the Michelson configuration of the interferometer. Figure 3 shows measured FEL beam spectra depending on detuning lengths of the FEL cavity. Measured results of the coherence lengths of the FEL micro-bunches for the detuning lengths of 0 and -0.8 mm from the resonance position of the FEL optical cavity are shown in left and right insets of the figure, respectively. The FWHM of the FEL line width is between 0.7 μm to 2 μm, which corresponds to 0.4-1.2% of the wavelength. The measured coherence length from the interferogram is between 10 mm to 16 mm in FWHM, which corresponds to the FEL bunch length of 25-40 ps (8-12 mm, FWHM) in the case of the Gaussian-shaped pulse. The bunch length from the coherence length measurement agrees well with the estimation of the FEL bunch length from the calculated value of the electron beam bunch.

The spatial distribution of the FEL beam was measured on the experimental stage as shown in Ref. [10]. The results show the distribution of the THz FEL beam is near Gaussian shape. We have focused the beam having spot size of 7 mm and wavelength of 110 mm with a parabola mirror (F/2). The focal length of the mirror is 50 mm. The measured beam waist at the focal point is 0.3 mm, which is close to value of the diffraction limitation from the 7-mm-diameter THz FEL beam.

We could understand that our THz FEL beam has excellent performance in power stability, polarization, spectral width, spatial distribution and wavefront. We hope that the THz radiation could be used for the advanced application of THz imaging for 3-D coherence tomography.

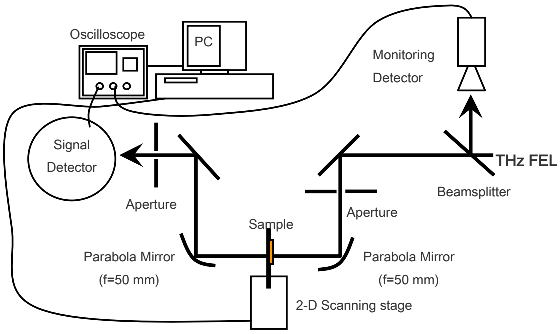

Figure 4: Schematics of the experimental setup for THz transmitted imaging with 2-D scanning of the samples.

2-D THZ IMAGING

Figure 4 shows schematics of the experimental setup for THz transmitted imaging with 2-D scanning of the samples. The 2-D scanning and data acquisition are automatically performed by a personal computer with a controller. For the first experiment on the THz imaging, we did not perform spectral study on the sample. Therefore the used wavelength for the THz imaging experiment was not optimised.

The first sample of 2-D THz imaging with our FEL was a microchip as shown in Fig. 5. From the experiment we could find the dynamic range of the THz imaging is much bigger than that of the usual vision recognition by human eyes. Even the dark part of the THz imaging inside the chip contains information on its structure. Figure 6 shows a transmitted THz imaging through an invisible paper box containing metal and silicon rings. We could see the shape of the rings clearly. Additionally the density information inside the silicon ring could be measured by the THz radiation, which means that the big dynamic range is very useful to recognize the nature of sample with THz spectral information. Without any additional processing of the imaging data, we could get the dynamic range of 10^5 for the measurements.

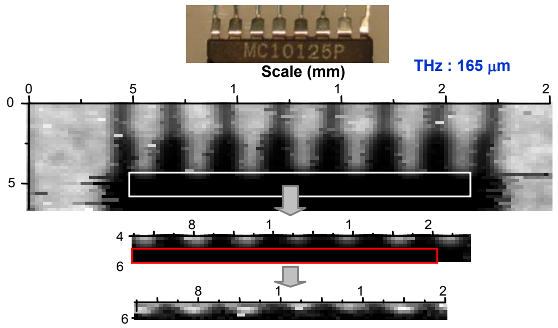

Figure 5: 2-D THz imaging of a microchip. From the experiment we could find the dynamic range of the THz imaging is much bigger than that of the usual vision recognition by human eyes. Even the dark part of the THz imaging inside the chip contains information on its structure.

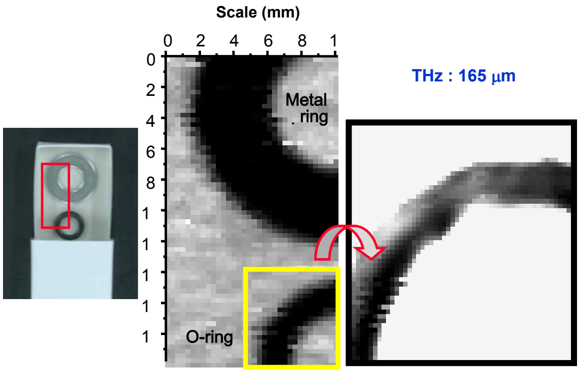

Figure 6: Transmitted THz imaging through an invisible paper box containing metal and silicon rings

Figure 7 shows a THz imaging of a gingko leaf, which is compared with a visible transmitted imaging. You can see the difference between the visible and THz imaging clearly. The main difference is caused by 10^3-10^4 times difference in absorption coefficient of liquid water between the two frequencies.

We are constructing a fast imaging system with a single micropulse of the THz beam by using the electro-optic (EO) detection and switching method. The linearly polarized visible or IR laser beam is collinearly incident to the EO crystal with the THz beam. The image of the THz beam is transferred to the visible or IR laser beam and the transferred image can be captured by an intensified CCD camera.

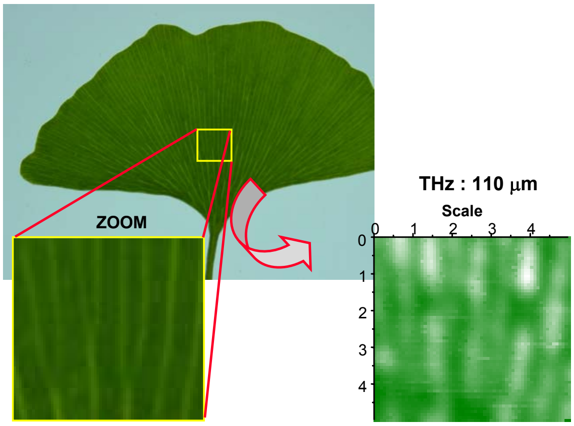

Fig. 7. Transmitted THz imaging of a gingko leaf, which is compared with a visible transmitted imaging.

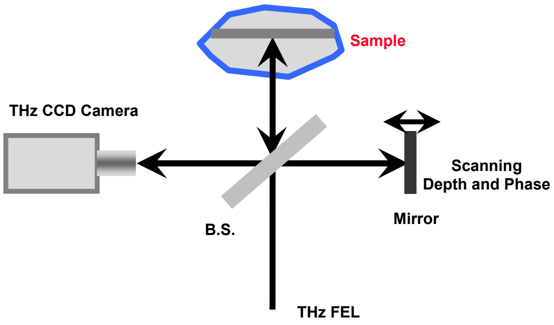

Figure 8: Schematics of the coherent THz tomography.

PROPOSAL FOR COHERENT 3-D THZ TOMOGRAPHY

The main difficulty of the THz tomography for medical application is the huge absorption of the radiation by liquid water which is the major constitution of human body. To get the information from inner part of living sample, we should remove the relatively strong signal scattered from the surface or near the surface of the sample. The most simple and effective way to get weak signal from strong background is to modulate the amplitude of the signal with the frequency which we can measure.

We have proposed a coherent 3-D THz tomography technique by using the method of holography. Figure 8 shows schematics of the coherent THz tomography. The THz FEL beam is divided into illuminating and reference beams. By using the short-pulsed feature of the THz FEL beam and controlling the optical path of the reference beam, we can select a certain cross-section inside the sample to make a hologram. By changing the optical path of the reference beam minutely, we can get modulating signal at fixed point of the hologram.

The idea is similar with optical coherence tomography (OCT) which uses optical range source. But in this technique, the light source has broad-band spectrum to reduce the resolution in depth up to ~μm. The light is focused on a point. And by modulating the path difference of reference beam, the absolute distance of depth is measured by the interference of the white light. Usually they get imaging information by scanning through x, y, and z. As you can see the detailed phase information of the interference is not important in the OCT technique. In our case, the THz FEL is narrow-band coherent source. The coherence length of the FEL beam is same as the pulse length, which is 8-12 mm as shown in Fig. 3. If we make and measure hologram with the beam, we could get the information of the depth less than the coherence length. With THz range light, it is much easier to get the phase information of the interference. And we do not need to get the full phase information through the coherence length because we only need the relative phase information among the points in imaging plane. If we have high power, coherent source of the THz light and sensitive measuring 2-D device for the THz light, we could get 3-D tomography of the living species with THz spectroscopic information.

CONCLUSION

We have developed a compact THz FEL and the main activity of its application for THz imaging is introduced in this paper. The FEL beam showed good performance in pulse-energy stability, polarization, spectrum and spatial distribution. We could get the 2-D imaging of various materials with the THz FEL beam. To perform spectroscopic imaging, we will develop a Fourier transform spectrometer for THz range. The main idea for 3-D coherent THz tomography is proposed and discussed briefly. We hope to develop the technique for bio-medical application or non-destructive inspection.

ACKNOWLEDGEMENTS

This work was supported by Korea Research Foundation Grant (KRF-2003-042-D00195).

REFERENCES

[1] Rudeger Kohler, et al., Nature, 417 (2002) 156.
[2] Kodo Kawase, et al., Appl. Phys. Lett. 78 (2001) 2819.
[3] Q. Wu and X.-C. Zhang, Appl. Phys. Lett. 67, (1995) 3523.
[4] M. Abo-Bakr, et al., Phys. Rev. Lett. 88 (2003) 254801.
[5] Y.U. Jeong, et al., Nucl. Instr. and Meth. A 475 (2001) 47.
[6] D.M. Mittleman, et al., Appl. Phys. B 68 (1999) 1085.
[7] K. Kawase, et al., Opt. Express 11 (2003) 2549.
[8] T. Loffler, et al., Opt. Express 9 (2001) 616.
[9] Y.U. Jeong, et al., Nucl. Instr. and Meth. A 507 (2003) 125.
[10] Y.U. Jeong, et al., Nucl. Instr. and Meth. A 528 (2004) 88.